

Alma Mater Studiorum Università di Bologna
Archivio istituzionale della ricerca

A 3D brute-force algorithm for the optimum cutting pattern of dimension stone quarries

This is the final peer-reviewed author's accepted manuscript (postprint) of the following publication:

Published Version:

Elkarmoty M, Bondua' S, Bruno R (2020). A 3D brute-force algorithm for the optimum cutting pattern of dimension stone quarries. RESOURCES POLICY, 68, 1-10 [10.1016/j.resourpol.2020.101761].

Availability:

This version is available at: <https://hdl.handle.net/11585/785334> since: 2020-12-23

Published:

DOI: <http://doi.org/10.1016/j.resourpol.2020.101761>

Terms of use:

Some rights reserved. The terms and conditions for the reuse of this version of the manuscript are specified in the publishing policy. For all terms of use and more information see the publisher's website.

This item was downloaded from IRIS Università di Bologna (<https://cris.unibo.it/>).
When citing, please refer to the published version.

(Article begins on next page)

1 **A 3D brute-force algorithm for the optimum cutting pattern of dimension stone quarries**

2

3 Mohamed Elkarmoty ^{a,b}, Stefano Bondua^c, Roberto Bruno^d

4

5

6 ^a Lecturer, Cairo University, Faculty of Engineering, Department of Mining, Petroleum, and Metallurgical
7 Engineering, 12316, Giza, Egypt

8

9 ^bPostdoc researcher, University of Bologna, School of Engineering and Architecture, Department of Civil,
10 Chemical, Environmental and Materials Engineering, Geo-resources Group, Via Terracini 28, 40131
11 Bologna, Italy, mohamed.elkarmoty2@unibo.it (corresponding author)

12

13 ^c Assistant Professor, University of Bologna, School of Engineering and Architecture, Department of Civil,
14 Chemical, Environmental and Materials Engineering, Geo-resources Group, Via Terracini 28, 40131
15 Bologna, Italy, stefano.bondua@unibo.it

16

17 ^d Associate Professor, University of Bologna, School of Engineering and Architecture, Department of Civil,
18 Chemical, Environmental and Materials Engineering, Geo-resources Group, Via Terracini 28, 40131
19 Bologna, Italy, stefano.bondua@unibo.it

20

21 **Abstract**

22 This paper presents a 3D algorithm for finding the optimum cutting direction in ornamental stone quarries
23 aiming at maximizing the recovery ratio of blocks through tackling the fracture problem that causes material
24 and economic losses. The presented algorithm is based on 3D deterministic fracture modeling or mapping
25 data and considers new parameters: i) displacement of the cutting grid; (ii) material lost by quarrying; (iii)
26 irregularity of the tested area; (iv) and subdivision of large quarrying area. The algorithm searches for the
27 optimum cutting direction and displacement of the cutting grid that maximizes the number of non-fractured
28 blocks. The algorithm was coded in a software package named BlockCutOpt. This paper presents
29 BlockCutOpt results applied in two case studies of different characteristics. The first case study was a
30 limestone bench where fractures were modeled deterministically using Ground Penetrating Radar (GPR)
31 survey. The second case study was in a very large area of granite quarrying zone where the regional
32 fractures were mapped using the aerial photogrammetry method (literature data). BlockCutOpt was found
33 as a fast tool for finding the optimum cutting pattern in the presented case studies. The results showed that
34 the optimum cutting direction of blocks can vertically (within different strata) and horizontally (within very
35 large scale area) vary, giving geometric information about the cutting grid design that optimizes the number
36 of non-fractured blocks.

37 **Keywords**

38 Sustainable quarrying; 3D optimization algorithm; Dimension stone; Recovery maximization; Waste
39 minimization

40 **1. Introduction and review**

41 Dimension stones are natural non-renewable resources that have to be quarried sustainably for
42 environmental and economic reasons (Carvalho et al., 2018). Stone quarrying industry should satisfy the
43 fundamental values of geoethics which include sustainability, environmental impact, economic
44 development (Careddu et al., 2019). Several works have studied the economic and environmental
45 sustainability of the dimension stone sector (Careddu, 2019; Careddu et al., 2013; Careddu and Siotto, 2011;
46 Macedo et al., 2017). Commercially, ornamental stones are considered as main economic resources for
47 many countries overall the world (Montani, 2008). However, about two-thirds of the ornamental stone
48 exploited material is waste whilst one-third goes to the market (Montani, 2003).

49 Natural rock discontinuities play a significant role in the profitability of ornamental stone quarries. The
50 exploitability of an ornamental stone deposit refers to the possibility of cutting non-fractured commercial-
51 size blocks from quarries (Carvalho et al., 2008). Among the others, discontinuities are one of the main

52 causes of waste production in the quarrying industry. Discontinuities occur in different geologic forms,
53 classes and dimensions as given in detail in (Gillespie et al., 2011). The profitability of ornamental stone
54 quarry can be optimized by minimizing waste production and maximizing the bulk extraction volume of
55 non-fractured commercial-size blocks (production optimization).

56 Fractures and discontinuities are natural rock-break surfaces that form natural rock blocks or can be named
57 in-situ blocks (Lu and Latham, 1999) whose size depends on spacing and number of discontinuities (ISRM,
58 1979). Geo-structurally speaking, the spacing of fractures is the most critical parameter affecting quarrying.
59 Generally, a larger fracture set spacing exhibits a larger amount and volume of extracted non-fractured
60 commercial-size blocks.

61 Several literature works presented geometric or stochastic methods to identify the geometry and quantify
62 the volume of natural blocks for mining and geoenvironmental purposes (e.g. Cho et al., 2012; Elmouttie and
63 Poropat, 2012; Turanboy, 2010; Turanboy and Ülker, 2008; Yarahmadi et al., 2015, 2014). The majority
64 of these previous works were based on the traditional manual method of fracture survey which has well-
65 known drawbacks (Assali et al., 2014; Kemeny and Post, 2003).

66 The estimation of natural rock blocks size and shape can be used for preliminary reserves estimation and
67 quantification in quarries, especially when the calculation of the maximum largest cuboid (Ülker and
68 Turanboy, 2009) or of the marketable block size (Mutlutürk, 2007) inside natural rock block can be
69 accomplished. Mosch et al., 2011, developed a software package, named 3D-BlockExpert, that can identify
70 and compute the volumes of the natural-formed blocks. 3D-BlockExpert can generate a derived 2D section
71 inside the rock body, from two selected parallel sections, to visualize the natural blocks' geometry. This
72 helps the user operator of the program to optically determines the most suitable arrangement of different
73 block sizes inside a derived 2D section (Mosch et al., 2011; Sousa et al., 2017). For the bench scale
74 quarrying, the approaches of natural blocks identification cannot be adopted to the quarrying logic, since
75 the orientation of the quantified/identified natural blocks may or may not be consistent with the typical
76 cutting strategy (continuous cutting direction for the same size of blocks quarried) in benches which is
77 practically non-changeable for quite large areas. Moreover, these approaches model fractures as planes with
78 finite persistence based on the data of the main fracture sets surveyed by the manual method which may
79 entail errors in identifying the actual natural blocks geometry.

80 For production optimization, the characterization of the deposit quality needs to be assessed. Geostatistical
81 methods give indices estimation for ornamental stone deposits (e.g. Taboada et al., 1999, 1997; Tercan and
82 Özçelik, 2000), however, the geostatistical methods are still far from the production optimization point of
83 view in this paper. Production optimization of ornamental stone deposits, in this paper, concerns finding

84 the optimum cutting direction of equal-sized blocks from benches of quarries, based on 3D deterministic
85 fracture modeling or fracture mapping as well, aiming at maximizing the production recovery ratio and/or
86 revenue when economic data are available. The approach in this paper is different than those which find
87 the optimal cutting direction based on geo-mechanical parameters of the deposit (Deliormanli and Maerz,
88 2016; Yarahmadi et al., 2017).

89 Optimization of ornamental stone production recovery was introduced in 2D, for the first time, graphically,
90 by (Tomasic, 1994) who illustrated that the production recovery is controlled by the block size, the spacing
91 of fractures, and the orientation of blocks. However, the graphical 2D application in the work of (Tomasic,
92 1994) was on an orthogonal vertical profile along a working bench and with considering different block
93 sizes, which is not coherent with the actual quarrying applicability.

94 The most noticeable contributions in 3D production optimization of ornamental stone deposits are the work
95 done by (Fernández-de Arriba et al., 2013) and (Yarahmadi et al., 2018). Fernández-de Arriba et al., 2013,
96 developed a numerical optimization algorithm programmed in a software package using the C#
97 programming language and named CUTROCK. The CUTROCK method is based on using the data (dip
98 angle, dip direction, and spacing) of three fracture families, assumed persistent and continuous planes, to
99 identify the volume of the maximum block bounded in the natural block inside the spatial data of the three
100 fractures families. A mesh of blocks with the desired dimensions is then generated in a parallelepiped form
101 and inside the maximum block. The final aim of this method was to find the optimum cutting orientation
102 within the mesh generated to maximize the yield. Field studies of several works have shown that fracture
103 families often occur in two or three prominent families and one or more minor families; in addition random
104 joints may be present (Palmström, 1995). This may cause errors in the optimization result of this method,
105 with a limitation of non-workability in case of the presence of a fracture set greater of the main three fracture
106 families.

107 Yarahmadi et al., 2018, improved the previous methods within two directions: (i) natural blocks
108 identification and classification numerically and (ii) production optimization. This work was coded in a
109 software package, using the MATLAB environment, and named 3D-QuarryOptimizer. Firstly, natural
110 block identification was improved by assuming random discontinuities with finite persistence and fracture
111 families while considering block shape factor. The block shape factor is a classification measure of the
112 shape quality and was defined as the ratio of the surface area of a representative rectangular block (with the
113 same volume as the given natural block) to the surface area of the natural block. The block shape factor
114 shows how much an irregularly shaped block is similar to an equal volume rectangular block and does not
115 provide information about the 3D orientation of the block, but it is an important aspect of the quarrying
116 suitability.

117 Regarding the optimization, 3D-QuarryOptimizer performs optimization within two scales: analysis of
118 quarrying direction on a large scale, based on the main fracture families' data, and cutting the interval in a
119 face on a small scale Large Volume Blocks (LVB): LVB (named in Italian language: *bancata*), loosened
120 by means of primary cuts, from which commercial sizes of blocks are cut. At small-scale optimization, a
121 genetic algorithm was used to find the best variable cutting intervals to cut blocks from a LVB. This is
122 theoretically an innovative optimization method; however, practically the cutting interval in large-scale
123 benches usually occurs with fixed distances and often occurs as well in large blocks.

124 On the other hand, the objective of the large-scale optimization algorithm, in 3D-QuarryOptimizer, was to
125 maximize the volume of the extracted blocks bounded in a mesh of blocks. Accordingly, several blocks'
126 classes of different volumes and shapes can be assessed to compute the economic value of each class. The
127 optimization algorithm presented in this paper can find the optimum commercial-size of the block, that can
128 be extracted from a bench, which maximizes the recovery ratio when several sizes are tested.

129 As given by (Reina and Loi, 2015), the blocks are classified into three classes, based on the rock material
130 and the geometric shape: (i) first class blocks have commercial size with six regularly-shaped sides (known
131 as blocks); (ii) second class blocks whose one or more faces are not regular (called "half blocks"), (iii) and
132 third class blocks which do not have a regular shape (known as "unformed"). Hereby, in this paper, the
133 optimization targets only to the first class blocks and the method can be applied following the current
134 quarrying routine.

135 The presented quarrying optimization algorithm, in this paper, decreases the gap between the previous
136 methods and improves the optimization concepts considering the practical aspects. The main features of
137 the presented optimization algorithm are listed as follows:

- 138 • The algorithm can work using any source of fracture data. Fracture surveys are usually performed
139 with the classical manual method, GPR, laser scanner, aerial and terrestrial photogrammetry. The
140 modeled fractures must be encoded in the Polygon File Format files (PLY) (Bourke P., 2011). The
141 results uncertainty may be minimized when using a 3D deterministic fracture model (Elkarmoty et
142 al., 2018b, 2017a).
- 143 • No natural block identification algorithms are required and there are no restrictions on the number
144 of fracture sets.
- 145 • The algorithm can work for a large scale bench or for a face on a small scale (LVB).
- 146 • The wasted material caused by the cutting method is newly considered in the algorithm.
- 147 • Providing a new option of dividing the tested area into several sub-divisions of quarrying zones.
- 148 • Introducing the horizontal displacements of the cutting grid of blocks as an optimization parameter.

149

150 2. Methodology

151

152 Accurate design and production plan of the cutting areas of non-fractured blocks can decrease the amount
153 of waste, improving quarrying sustainability. As fractures are generally modeled as three-dimensional
154 planes, there will be a potential risk of inaccuracy and, consequently, forming of waste material during
155 quarrying operation. While modelling fractures deterministically as irregular 3D surfaces as close as
156 possible to reality may lead to the optimal minimization of waste (Elkarmoty et al., 2018a, 2017a, 2017b).
157 The optimum cutting direction can be determined by an optimization algorithm through finding orientation,
158 interval, and other cutting parameters allowing to maximize the number of non-fractured blocks.

159 The authors of this paper have recently developed an algorithm for an optimized slab cutting from
160 ornamental stone blocks, named SlabCutOpt (Elkarmoty et al., 2020). The SlabCutOpt software was coded
161 in the C++ programming language. In this paper, it is presented a modification to the SlabCutOpt algorithm,
162 having adapted it to the quarrying logic to optimize the cutting of blocks from quarry benches. The adapted
163 algorithm in this paper was named “BlockCutOpt” referring to Block Cutting Optimization.

164 BlockCutOpt, similarly to SlabCutOpt, searches for the intersection between fractures and blocks defined
165 in a 3D cutting grid, initiated from the geometric center of the tested area. The 3D cutting grid of blocks is
166 then rotated, with a fixed given step of the cutting direction. For each simulated cutting direction, the 3D
167 cutting grid is displaced horizontally (dx and dy), within a given domain, to test several designs of cutting
168 grids as well, outputting the number of non-intersected blocks with full dimension inside the tested area.
169 Following, the recovery ration can be calculated by Eq. 1. The optimum revenue can be estimated as well
170 when the selling prices of several tested sizes of blocks are available, following the work presented in
171 (Elkarmoty et al., 2020).

$$172 \text{ recovery (\%)} = \frac{\text{volume of non-intersected blocks with full dimension inside the rock body studied} \times 100}{\text{total volume of the rock body studied}} \quad (1)$$

173 Hence, the presented method uses a developed brute-force algorithm, searching for not only the possible
174 cutting directions but also for the corresponding possible designs of the cutting grid. A simplified graph in
175 Fig. 1 illustrates the used method in 2D.

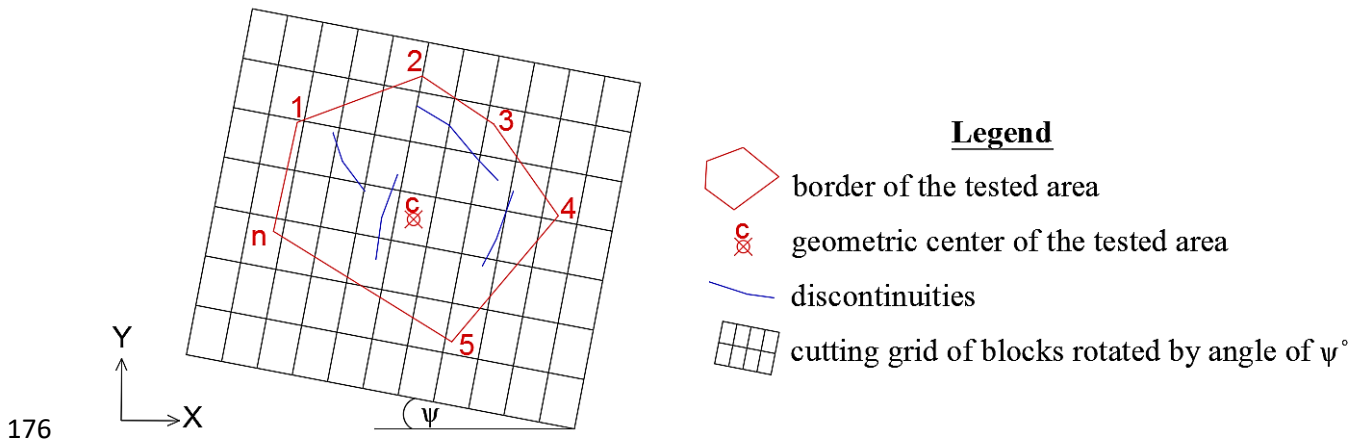


Fig. 1. A 2D illustrative sketch for the used method.

178 BlockCutOpt contains the same concept of the 3D cutting grid domain in SlabCutOpt. The dimensions of
 179 slabs were replaced by the dimensions of blocks and the surveyed block body was replaced by the surveyed
 180 bench body. The thickness of the saw was replaced by the thickness of lost material due to quarrying, named
 181 in the algorithm “material-lost-by-quarrying”. The main adaptations or modifications done in BlockCutOpt
 182 are listed below:

- 183
- Only the horizontal rotation is considered (ψ) which is the cutting/quarrying direction ranging from
 184 0.0° to 180° .
 - No vertical displacement (dz) of the 3D cutting grid of blocks is considered.
 - The tested quarrying area can be in any geometric shape: a regular shape or a concave/convex
 187 polygon.
 - Optionally, in case of large area computation, the tested area can be divided into equal sub-divisions
 188 of quarrying. The sub-areas/sub-divisions are identified in the algorithm by $(m_x=i, m_y=j)$, where i is
 189 the number of the sub-areas in the X direction and j is the number of the sub-areas in the Y direction.
 190 For example, when an area is computed in the algorithm using $(m_x=2, m_y=2)$, this means that this
 191 area contains four sub-divisions of quarrying zones defined by $(i=1, j=1)$, $(i=2, j=1)$, $(i=1, j=2)$, and
 192 $(i=2, j=2)$. If $(m_x=1, m_y=1)$, the algorithm will work on a single tested area without sub-areas.
 193

194 The input/output files of BlockCutOpt have the same features of the input/output files of SlabCutOpt,
 195 considering some differences in the file containing the input parameters, named BlockCutOpt.par. In
 196 addition, in case of using the sub-division of the tested area option, the Results.log file of BlockCutOpt lists
 197 the results separately for each sub-division zone.

198 3. Case studies and results

199 3.1. Limestone quarry of Italy

200 **3.1.1. Input data**

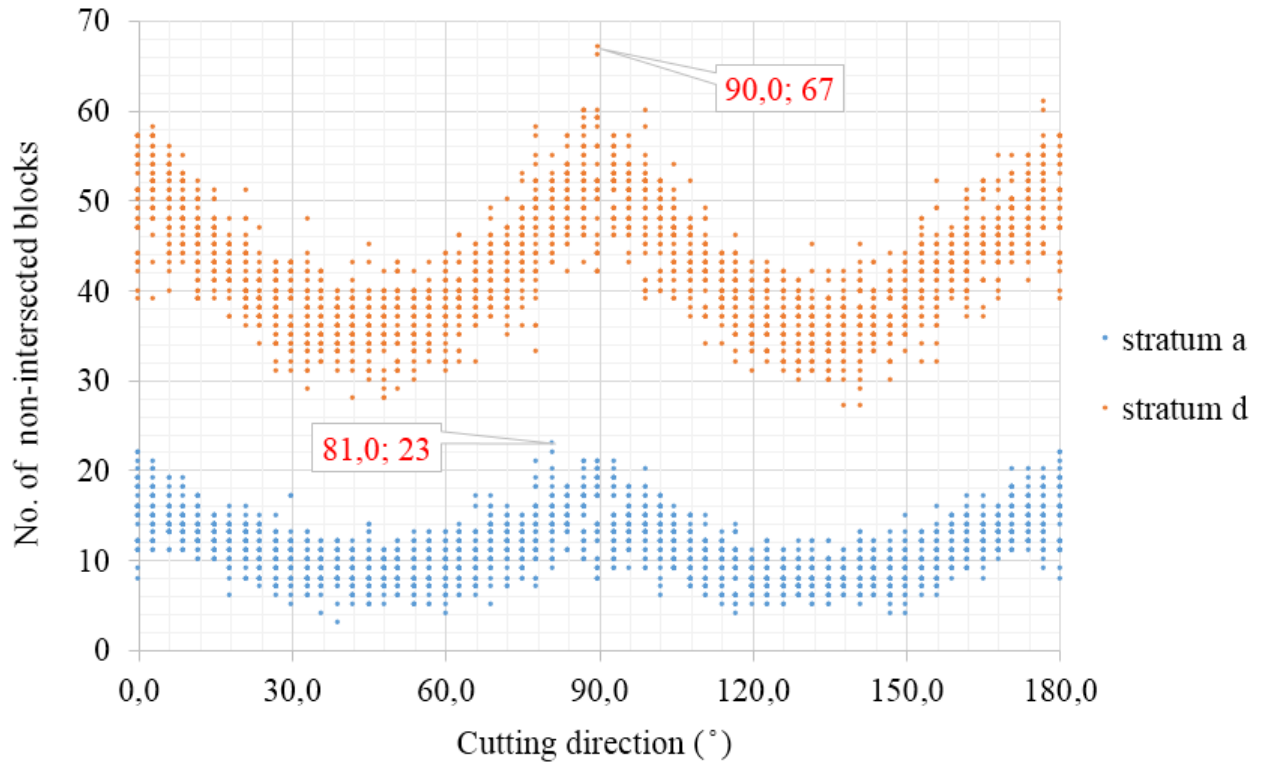
201 BlockCutOpt was applied to a bench of limestone quarry where fractures were modeled deterministically
202 in 3D based on Ground Penetrating Radar (GPR) survey. The site description and the fracture model are
203 presented in detail in (Elkarmoty et al., 2018b) .The final goal of applying BlockCutOpt software on this
204 case study was to investigate the effect of fractures modeling as 3D surfaces on the production optimization
205 results. In this case study, one commercial size block has been tested in BlockCutOpt. By personal
206 communication with the quarry technical manager, the preferred block dimensions reported are 3.0 m
207 length, 2.0 m width and the thickness of the block is limited to the thickness of the strata. In this case study,
208 the surveyed bench had four strata (a, b, c, and d), as shown in (Elkarmoty et al., 2018b). BlockCutOpt was
209 used to test the referred block size with its relevant thickness for each stratum in order to find the solutions
210 for the maximum number of non-intersected blocks and the related optimum recovery.

211 In this case study, the cutting direction has been tested with an angle step of 3.0° and using a horizontal
212 displacements of 0.5 m in the X and in the Y directions for the 3D cutting grid of blocks. The thickness of
213 the material-lost-by-quarrying was assumed 5.0 cm. See Appendix A as an example for an input file for
214 this case study considering a no sub-divisions of the tested area.

215 **3.1.2. Optimization results**

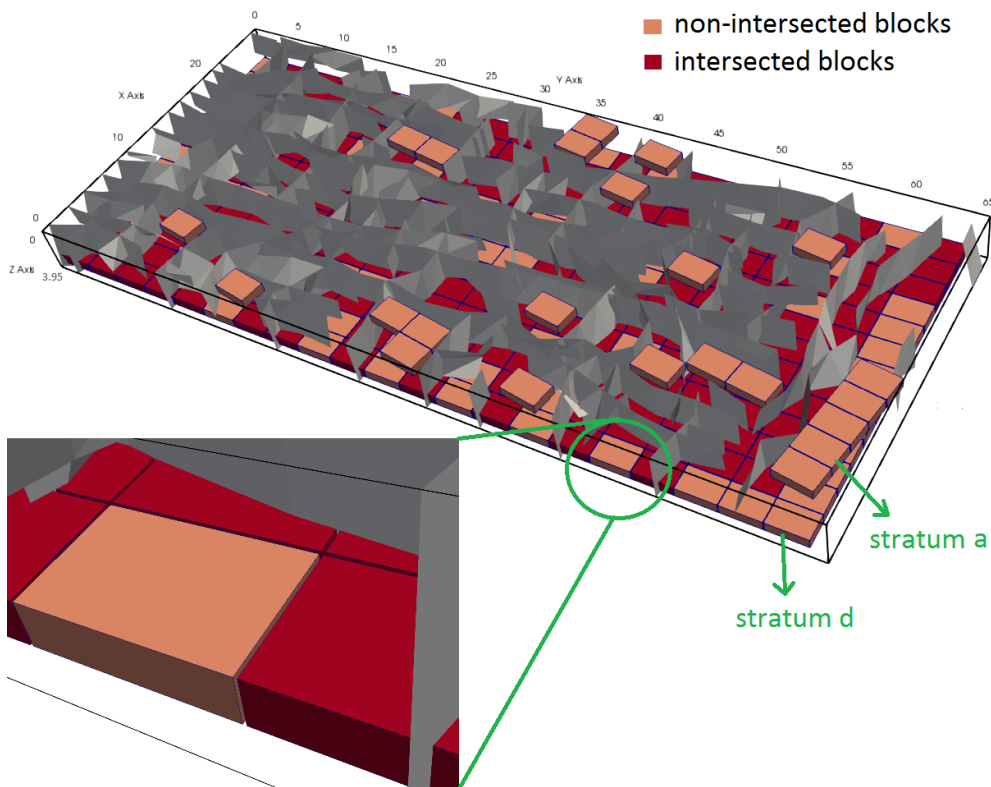
216 The results of applying BlockCutOpt to the different blocks sizes provided that the maximum number of
217 non-intersected blocks were found variable with the cutting direction, and also with the displacements for
218 each cutting direction tested. Mainly this is due to modeling fractures as 3D surfaces allowing results change
219 between strata. A graphical representation for the results of Strata a and d are shown in Fig. 2 and visualized
220 in Fig. 3. The material lost by quarrying can be also observed in the zooming part of Fig. 3. For better
221 visualization of Stratum d in Fig. 3, the fractured/intersected blocks of Stratum a were hidden.

222 The time consumed to solve the problem by BlockCutOpt, for the four strata, was 11.0 minutes. This
223 considers selecting write_vtu=2 in the PAR file (parameter for writing only the maximum number of non-
224 intersected blocks), and using a computer of the following specifications: 64-bit operating system Windows
225 7, processor Intel(R) Core (TM) i5-4460 CPU @ 3.20 GHz, and installed memory (RAM) 8.00 GB.



226

227 Fig. 2. The optimization results of Strata a and d.



228

229 Fig. 3. 3D visualization of the optimum solutions, for Strata a and d.

230 The algorithm results give the optimum solution in terms of non-fractured blocks, further consideration
 231 must be taken in account, such as the comparison between several block sizes and the market values (selling
 232 prices) that usually depend on sizes, as presented in (Elkarmoty et al., 2020). Table 1 summarizes the
 233 optimization results of this case study. The total number of non-intersected blocks in the bulk volume of
 234 the bench was 150 blocks leading to a bulk recovery ratio of 11.4 %. It is worth mentioning that the cutting
 235 direction actually used in this bench was 0.0 ° (traditionally fixed for all the strata) which is found not
 236 consistent with the optimization results.

237 **Table 1**
 238 A summary of optimization results for each stratum.

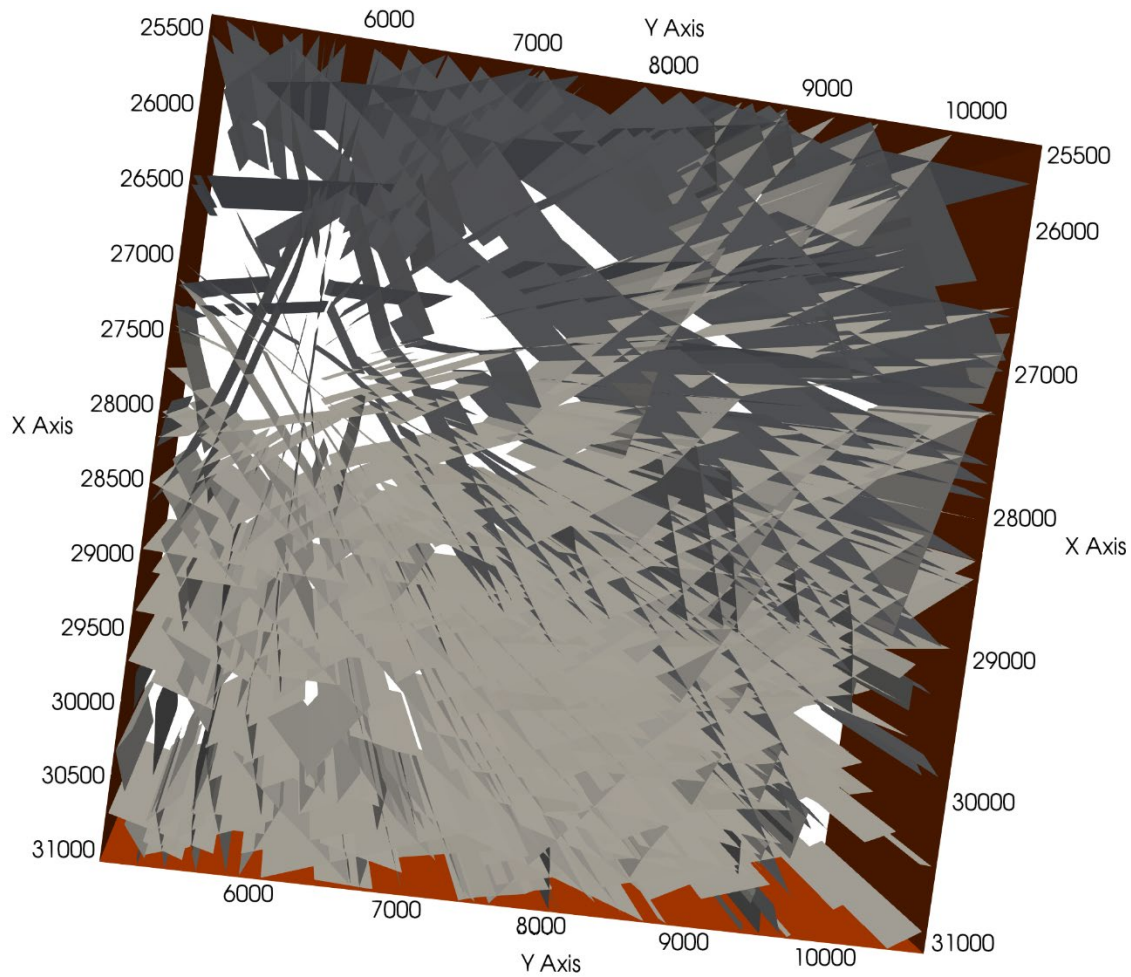
stratum	max. No. of non-intersected blocks	max. recovery (%)	dx (m)	dy (m)	cutting direction (°)
a	23	7.86	-0.51	-1.01	81.0
b	23	7.68	-1.01	0.99	90.0
c	37	12.65	-1.01	0.99	90.0
d	67	22.91	0.99	0.99	90.0

239
 240 **3.2. Granite extraction area, Portugal - photogrammetry data**

241 **3.2.1. Input data**

242 The objective of this case study was to verify and validate the use of BlockCutOpt in a very large scale
 243 quarrying area, for the target of a long-term optimization plan. In particular, when a large area of
 244 exploitation can be divided into sub-areas where the optimum cutting direction varies. Published data was
 245 used as input in this case study. A map of regional fracturing (figure 7 of (Sousa et al., 2016)), obtained by
 246 aerial photogrammetry, in a large quarrying zone of granite, was reproduced. The fracture map in (figure 7
 247 of (Sousa et al., 2016)) has been converted in a format readable by BlockCutOpt through manual picking
 248 and automatic exporting of fracture coordinates to an excel worksheet using the AutoCad add-on utility
 249 “click2xls”, which facilitated the transformation of the fracture data into a PLY file. The reproduced
 250 fractures map is visualized in Fig. 4. It was assumed that the whole fractures were vertical, persistent and
 251 continuous planes. It is worth mentioning that no horizontal fractures data were detected or considered for
 252 the map of the tested quarrying area.

253 The total area under study is 5650.6 X (m) x 5675.8 Y (m). The border of the studied zone in BlockCutOpt
 254 was assumed to be the same border of the original map. Since this case study is a very large scale area, the
 255 optimization results could be provided within the two possible options, the first considers the sub-division
 256 option and the second considers the whole area.



257

258 Fig. 4: Oriented 3D visualization of the fracture data, reproduced from (figure 7 of (Sousa et al., 2016)).

259

260 For the application of BlockCutOpt in this case study, the tested size of the block was the LVB. This is the
 261 most common size cut in marble and granite quarries. The LVB volume is usually in the 1000s of m³ range:
 262 length of 20.0-30.0 m, width of 9.0-12.0 m, and height of 6.0-7.0 m (Ashmole and Motloun, 2008). The
 263 dimensions of a large block are generally determined considering the machinery limitations. However, in
 264 this case study, and since there are no more available data, the author simulated a size of LVB (Table 2)
 265 that has similar dimensions and volumes given by (Ashmole and Motloun, 2008).

266 **Table 2**

267 The dimensions of tested LVB in BlockCutOpt.

length, X(m)	width, Y(m)	height, Z(m)	volume (m ³)
21.0	9.0	6.0	1080.0

268

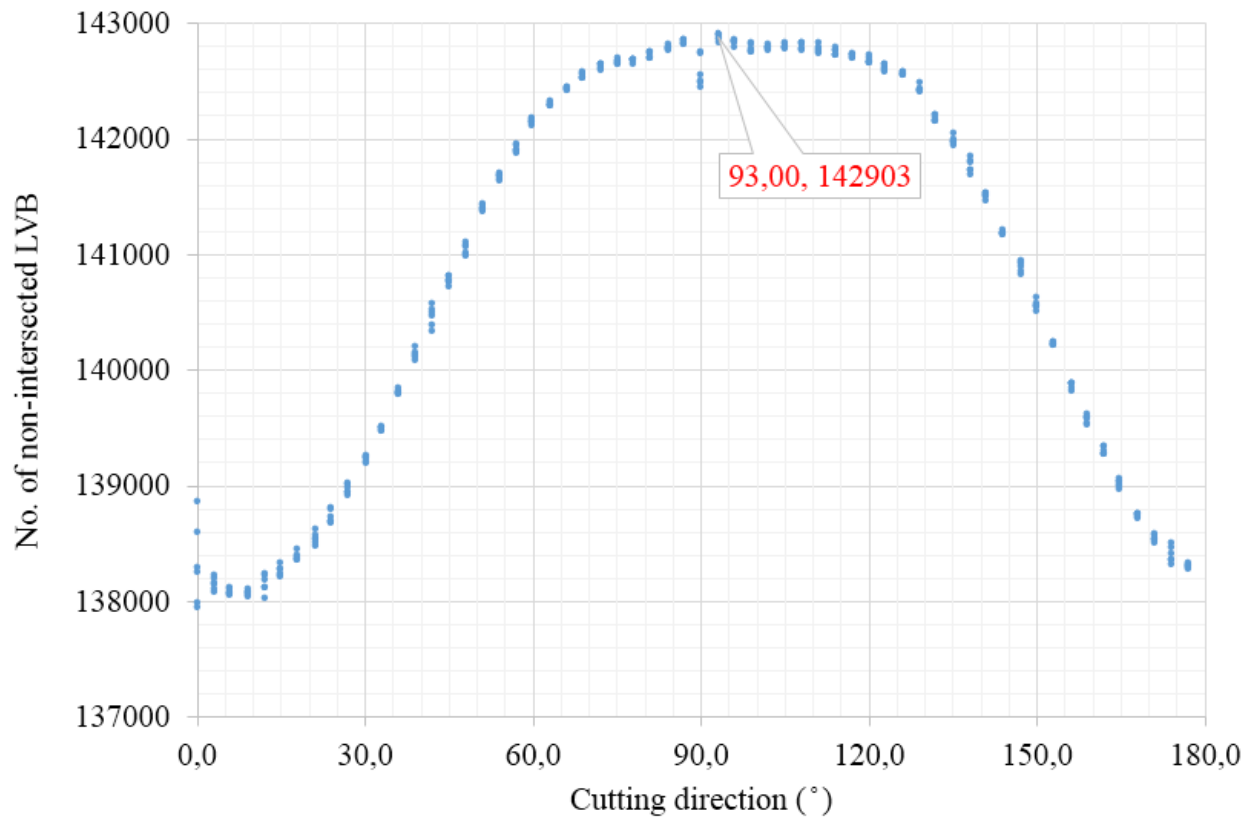
269

270 In this case study, the cutting direction will be tested within angles interval of 3.0° and using maximum
271 horizontal displacements of 7.0 m in the X direction and 5.0 m in the Y direction. The thickness of the
272 material lost by the cutting systems was set as 5.0 cm. See Appendix B as an example for an input file for
273 this case study considering the sub-division of the tested area.

274 **3.2.2. Optimization results**

275 Firstly, the results will be presented considering the non-division of the tested area. The results of applying
276 BlockCutOpt to the tested size of LVB is graphically presented in Fig. 5. It is found that the recovery ratio
277 changes with the cutting direction. For the tested angles of the cutting direction, BlockCutOpt finds
278 solutions for several displacements of the cutting grid. The variability range of the recovery ratio was
279 limited (80.40-83.29 %). The high recovery ratio was expected, in this case study due to the small surface
280 area of the LVB tested, compared to the quarrying area studied and the fracture data set, just about the main
281 fractures at the regional scale. The maximum number of non-intersected LVBS was found at the cutting
282 direction of 93.0° , at a displacement of $dx = -10.01$ m and $dy = 0.49$ m, providing the maximum recovery
283 of 83.29 %. The maximum number of non-intersected LVBS solution is visualized in Fig. 6 where the
284 cutting direction of the optimum solution is 93.0° . The time consumed by BlockCutOpt to solve the problem
285 was 26.0 hours, considering `write_vtu=2` in the PAR file, and using a computer of the following
286 specifications: 64-bit operating system Windows 10, a processor Intel i7-3770K CPU @ 3.7 GHz , and an
287 installed memory (RAM) of 8.00 GB.

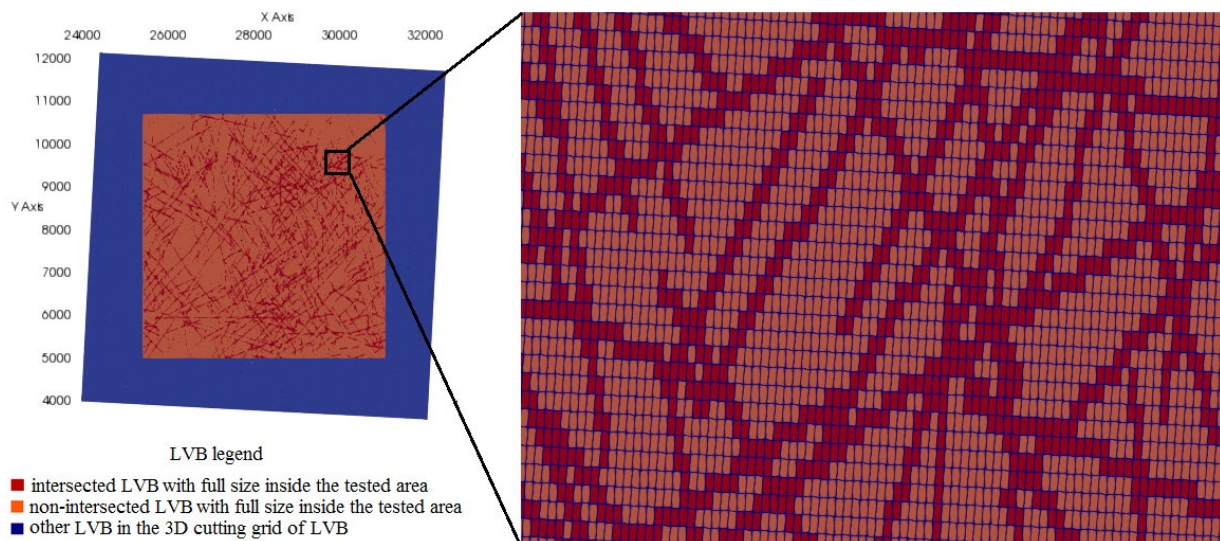
288



289

290 Fig. 5. The optimization results of the tested size of LVB, without sub-division, highlighting the optimum
 291 solution.

292



293

294 Fig. 6. Two-dimensional visualization of the optimum solution (non-intersected LVBs solution), without
 295 sub-division.

296

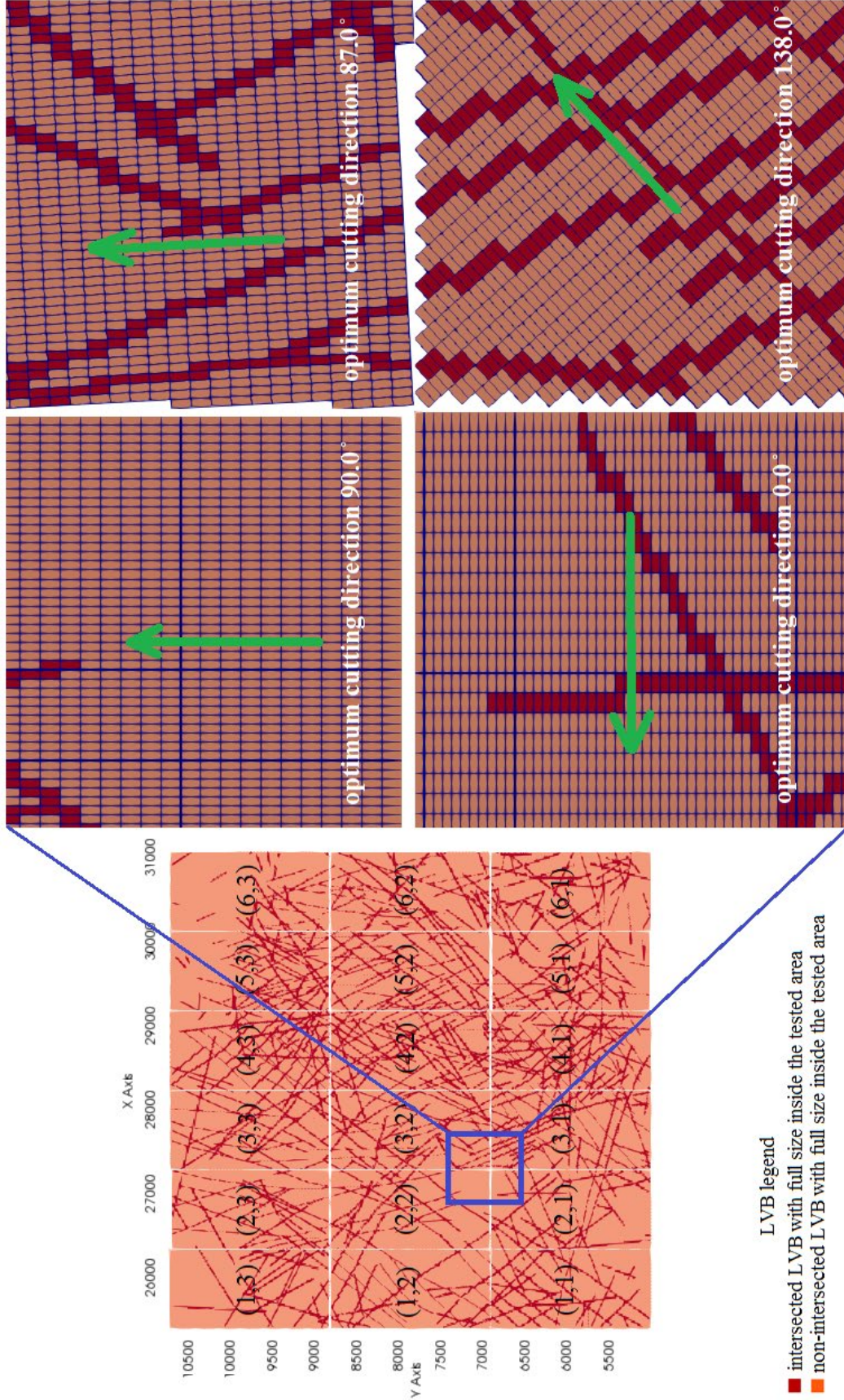
297 Considering the sub-division of the tested area, the whole tested area was firstly divided into 3 sub-areas of
 298 quarrying zones in the X direction and 2 sub-divisions of quarrying zones in the Y direction ($m_x=3, m_y=2$),
 299 leading to a total of 6 sub-divisions of quarrying zones. The computation results are shown in Table 3 for
 300 the 6 sub-divisions of quarrying zones. From the results in Table 3, it is shown that the maximum number
 301 of non-intersected blocks for the sub-division zones are found at different displacements, even if the
 302 optimum cutting direction of 90.0 is almost the predominant one. The maximum number of non-intersected
 303 LVBs, in all the sub-division zones, was 142701: less than in the without sub-division test, giving an overall
 304 optimum recovery of 83.17 %.

305 **Table 3**
 306 The optimization results for each sub-division quarrying zone ($m_x=3, m_y=2$).

i	j	max. No. of non-intersected LVBs	dx (m)	dy (m)	cutting direction (°)
1	1	25104	-3.01	-4.51	129.0
1	2	24718	-3.01	-4.51	90.0
2	1	21840	3.99	-4.51	90.0
2	2	22713	3.99	0.49	90.0
3	1	23744	-3.01	-4.51	90.0
3	2	24582	-3.01	0.49	90.0

307 For this case study, the use of sub-division zones shows a decrease of the maximum number of non-
 308 intersected blocks since the borders of the sub-division zones were acting as fractures. However, a
 309 noticeable variation of the optimum cutting direction for each sub-division quarrying zone is expected. This
 310 is logically obvious; nonetheless, BlockCutOpt can quantify and graphically visualize the results (using
 311 ParaView). A further test of increasing the sub-division zones was performed for ($m_x=6, m_y=3$). The results
 312 are visualized in Fig. 7 and summarized for each sub-division quarrying zone in Table 4. It is worth
 313 mentioning that the optimum cutting direction (93.0°) for the without sub-division test was not found in any
 314 optimum solution of the sub-division zones presented in both of Table 3 and Table 4.
 315

316



318 **Table 4**
 319 The optimization results for each sub-division quarrying zone (mx=6,my=3).

i	j	max. No. of non-intersected LVBs	dx (m)	dy (m)	cutting direction (°)
1	1	8123	-10.01	-4.51	0.0
1	2	8219	-10.01	-4.51	132.0
1	3	8514	-10.01	-4.51	0.0
2	1	8294	-10.01	-4.51	0.0
2	2	8374	-3.01	0.49	90.0
2	3	8076	-3.01	-4.51	90.0
3	1	7403	-3.01	0.49	138.0
3	2	7672	-3.01	-4.51	87.0
3	3	7971	-3.01	0.49	90.0
4	1	6956	-10.01	0.49	138.0
4	2	6970	-3.01	0.49	90.0
4	3	7295	-3.01	0.49	132.0
5	1	7870	-10.01	-4.51	90.0
5	2	7515	-10.01	0.49	90.0
5	3	7761	-10.01	0.49	90.0
6	1	8008	-10.01	-4.51	0.0
6	2	7837	-3.01	0.49	90.0
6	3	8854	-10.01	0.49	90.0

320
 321 It was noticed that the total number of non-intersected LVBs decreased (Table 5) with increasing the sub-
 322 division zones. This is due to the borders effect of the sub-division zones acted as additional “synthetic”
 323 fractures. The sub-division method can give better bulk recovery impact, in case a large area of quarrying
 324 shall be divided into sub-zones for planning, business, or geographic reasons. Given that, the optimum
 325 solution found for each sub-division zone is the one providing the best recovery for that area.

326 **Table 5**
 327 Comparison between the with and without sub-division solutions.

	without sub- division	sub-division (mx=3,my=2)	sub-division (mx=6,my=3)	sub-division (mx=9,my=4)
optimum recovery (%)	83.29	83.17	82.60	82.04
optimum No. of non-intersected LVBs	142903	142701	141712	140767

328

329 **4. Conclusions**

330 The presented algorithm allowed to find the optimum cutting direction in quarries that maximizes the
 331 number of non-fractured blocks or Large Volume Blocks (LVBs) and consequently the recovery ratio. The
 332 algorithm was successfully coded in the C++ programming language (named BlockCutOpt), allowing fast
 333 calculation and visualization of the results.

334 BlockCutOpt was applied in two case studies. The first one was a limestone bench where fractures were
 335 modeled deterministically based on GPR survey. The modeling of fractures as 3D surfaces plays a
 336 significant rule in the optimization results. The results of BlockCutOpt showed that the optimum cutting
 337 grid design (cutting direction and displacement) may vary vertically between strata deposited in the same
 338 bench providing consequently different maximum recovery ratios for each stratum. For this case study, as
 339 selling prices of different commercial-sizes blocks are variable, the BlockCutOpt can be used to find the
 340 optimum block size providing the maximum revenue as well.

341 The second case study was a granite deposit with a large area where regional fractures were mapped (in
 342 literature) by photogrammetry. BlockCutOpt proved its ability to solve a very large scale problem contains
 343 a huge number of blocks in a reasonable time of computation. In this case study, the problem was solved
 344 for a size of LVB from which commercial-size blocks cut. Therefore, the results in this case study are
 345 limited to the optimization of LVBS considering the limitations of the aerial mapping of fractures. The
 346 optimum cutting direction was found variable within the sub-divided zones. Increasing the number of the
 347 sub-divided zones led to increasing the variability of the optimum cutting directions and the displacements
 348 of the optimum cutting grids. The total optimum recovery slightly decreased, as compared to the non-
 349 division solution, when the number of sub-divisions of quarrying zones increased (the borders acted as
 350 synthetic fractures). However, the maximum recovery ratio found for each sub-division zone is significant
 351 when a large area shall be divided into sub-zones for planning, business or geographic reasons.
 352 Interestingly, the optimum cutting direction in the non-division solution could not be found in the whole
 353 sub-division solutions of (mx=3,my=2) (mx=6,my=3).

354 To conclude, the implementation of BlockCutOpt in the two case studies showed that optimum cutting
 355 direction of blocks can vary and that BlockCutOpt is able to provide geometric information about the cutting

356 grid of blocks that optimizes the resource exploitation, maximizing recovery and minimizing waste. For
357 future work, it is suggested to perform a field comparison study between the results obtained from
358 BlockCutOpt and the field results of cutting blocks from benches of quarries. Considering production costs
359 and energy saving aspects in the algorithm is recommended.

360 **Acknowledgements**

361 Thanks to the EU-METALIC II—ERASMUS MUNDUS program for funding the PhD scholarship of the
362 lead author. The authors are grateful to the Italian Ministry of Foreign Affairs and International Cooperation
363 for funding Mohamed Elkarmoty work to improve and continue the research topic in this paper. Many
364 thanks for Mr. Michele Augelli, “Augelli Marmi” quarrying company, for allowing the GPR measurements
365 in their quarry. Special thanks to Dr. Carlo Cormio (SERENGEO Srl, a spin-off company of University of
366 Bologna) for the technical suggestions provided.

367 **References**

368 Ashmole, I., Motloung, M., 2008. Dimension stone: the latest trends in exploration and production
369 technology., in: *The International Conference on Surface Mining 2008 – Challenges, Technology,*
370 *Systems and Solutions – Papers.* The Southern African Institute of Mining and Metallurgy,
371 Johannesburg, Republic of South Africa, pp. 35–70.

372 Assali, P., Grussenmeyer, P., Villemin, T., Pollet, N., Viguier, F., 2014. Surveying and modeling of rock
373 discontinuities by terrestrial laser scanning and photogrammetry: Semi-automatic approaches for
374 linear outcrop inspection. *J. Struct. Geol.* 66, 102–114. <https://doi.org/10.1016/j.jsg.2014.05.014>

375 Bourke P., 2011. PLY - Polygon File Format [WWW Document]. URL
376 <http://paulbourke.net/dataformats/ply/> (accessed 4.4.20).

377 Careddu, N., 2019. Dimension stones in the circular economy world. *Resour. Policy* 60, 243–245.
378 <https://doi.org/10.1016/j.resourpol.2019.01.012>

379 Careddu, N., Di Capua, G., Siotto, G., 2019. Dimension stone industry should meet the fundamental values
380 of geoethics. *Resour. Policy* 63. <https://doi.org/10.1016/j.resourpol.2019.101468>

381 Careddu, N., Siotto, G., 2011. Promoting ecological sustainable planning for natural stone quarrying . The
382 case of the Orosei Marble Producing Area in Eastern Sardinia. *Resour. Policy* 36, 304–314.
383 <https://doi.org/10.1016/j.resourpol.2011.07.002>

384 Careddu, N., Siotto, G., Siotto, R., Tilocca, C., 2013. From land fill to water, land and life : the creation of
385 the Centre for stone materials aimed at secondary processing. *Resour. Policy* 38, 258–265.

386 <https://doi.org/10.1016/j.resourpol.2013.05.001>

387 Carvalho, J., Lopes, C., Mateus, A., Martins, L., Goulão, M., 2018. Planning the future exploitation of
388 ornamental stones in Portugal using a weighed multi-dimensional approach. *Resour. Policy* 59, 298–
389 317. <https://doi.org/10.1016/j.resourpol.2018.08.001>

390 Carvalho, J.F., Henriques, P., Falé, P., Luís, G., 2008. Decision criteria for the exploration of ornamental-
391 stone deposits: Application to the marbles of the Portuguese Estremoz Anticline. *Int. J. Rock Mech.*
392 *Min. Sci.* 45, 1306–1319. <https://doi.org/10.1016/j.ijrmms.2008.01.005>

393 Cho, T.F., Lee, S.B., Won, K.S., 2012. Three-dimensional deterministic block analysis model for
394 information-oriented excavation design. *Int. J. Rock Mech. Min. Sci.* 55, 63–70.
395 <https://doi.org/10.1016/j.ijrmms.2012.05.003>

396 Deliormanli, A.H., Maerz, N.H., 2016. Stress Related Fracturing in Dimension Stone Quarries. *IOP Conf.*
397 *Ser. Earth Environ. Sci.* 44. <https://doi.org/10.1088/1755-1315/44/5/052020>

398 Elkarmoty, M., Bondu, S., Bruno, R., 2020. A 3D optimization algorithm for sustainable cutting of slabs
399 from ornamental stone blocks. *Resour. Policy* 65. <https://doi.org/10.1016/j.resourpol.2019.101533>

400 Elkarmoty, M., Colla, C., Gabrielli, E., Bonduà, S., Bruno, R., 2017a. Deterministic Three-dimensional
401 Rock Mass Fracture Modeling from Geo-radar Survey: A Case Study in a Sandstone Quarry in Italy.
402 *Environ. Eng. Geosci.* 23, 314–331. <https://doi.org/10.2113/gseegeosci.23.4.314>

403 Elkarmoty, M., Colla, C., Gabrielli, E., Kasmaeeyazdi, S., Tinti, F., Bonduà, S., Bruno, R., 2017b. Mapping
404 and modelling fractures using ground penetrating radar for ornamental stone assessment and recovery
405 optimization: Two case studies. *Mining-Geology-Petroleum Eng. Bull.* 32.
406 <https://doi.org/10.17794/rgn.2017.4.7>

407 Elkarmoty, M., Tinti, F., Kasmaeeyazdi, S., Bonduà, S., Bruno, R., 2018a. 3D modeling of discontinuities
408 using GPR in a commercial size ornamental limestone block. *Constr. Build. Mater.* 166, 81–86.
409 <https://doi.org/10.1016/j.conbuildmat.2018.01.091>

410 Elkarmoty, M., Tinti, F., Kasmaeeyazdi, S., Giannino, F., Bonduà, S., Bruno, R., 2018b. Implementation
411 of a fracture modeling strategy based on georadar survey in a large area of limestone quarry bench.
412 *Geosciences* 8, 1–15. <https://doi.org/10.3390/geosciences8120481>

413 Elmouttie, M.K., Poropat, G. V., 2012. A method to estimate in situ block size distribution. *Rock Mech.*
414 *Rock Eng.* 45, 401–407. <https://doi.org/10.1007/s00603-011-0175-0>

415 Fernández-de Arriba, M., Díaz-Fernández, M.E., González-Nicieza, C., Álvarez-Fernández, M.I., Álvarez-
416 Vigil, A.E., 2013. A computational algorithm for rock cutting optimisation from primary blocks.
417 *Comput. Geotech.* 50, 29–40. <https://doi.org/10.1016/j.compgeo.2012.11.010>

418 Gillespie, M.R., Barnes, R.P., Milodowski, A.E., 2011. British Geological Survey scheme for classifying
419 discontinuities and filings, British Geological Survey. Keyworth, Nottingham, England.

420 ISRM, 1979. Suggested methods for the quantitative description of discontinuities in rock masses. *Int. J.*
421 *Rock Mech. Min. Sci. Geomech. Abstr.* 15, 319–368. [https://doi.org/10.1016/0148-9062\(78\)91472-9](https://doi.org/10.1016/0148-9062(78)91472-9)

422 Kemeny, J., Post, R., 2003. Estimating three-dimensional rock discontinuity orientation from digital images
423 of fracture traces. *Comput. Geosci.* 29, 65–77. [https://doi.org/10.1016/S0098-3004\(02\)00106-1](https://doi.org/10.1016/S0098-3004(02)00106-1)

424 Lu, P., Latham, J.-P., 1999. Developments in the assessment of in-situ block size distributions of rock
425 masses. *Rock Mech. Rock Eng.* 32, 29–49. <https://doi.org/10.1007/s006030050042>

426 Macedo, D., Mori Junior, R., Pimentel Mizusaki, A.M., 2017. Sustainability strategies for dimension stones
427 industry based on Northwest region of Espírito Santo State, Brazil. *Resour. Policy* 52, 207–216.
428 <https://doi.org/10.1016/j.resourpol.2017.03.005>

429 Montani, C., 2008. *Stone 2008—world marketing handbook*. Faenza, Gruppo Editoriale Faenza Editrice,
430 Faenza.

431 Montani, C., 2003. *Stone 2002—world marketing handbook*. Gruppo Editoriale Faenza Editrice., Faenza,
432 Italy.

433 Mosch, S., Nikolayew, D., Ewiak, O., Siegesmund, S., 2011. Optimized extraction of dimension stone
434 blocks. *Environ. Earth Sci.* 63, 1911–1924. <https://doi.org/10.1007/s12665-010-0825-7>

435 Mutlutürk, M., 2007. Determining the amount of marketable blocks of dimensional stone before actual
436 extraction. *J. Min. Sci.* 43, 75–80. <https://doi.org/10.1007/s10913-007-0008-4>

437 Palmström, A., 1995. *RMi – a rock mass characterization system for rock engineering purposes*. PhD thesis,
438 Oslo University, Norway.

439 Reina, A., Loi, M., 2015. Environmental background in Apricena quarries (Apulia, Southern Italy), in:
440 Lollino, G., Manconi, A., Guzzetti, F., Culshaw, M., Bobrowsky, P., Luino, F. (Eds.), *Engineering*
441 *Geology for Society and Territory - Volume 5: Urban Geology, Sustainable Planning and Landscape*
442 *Exploitation*. Springer International Publishing, Switzerland, pp. 1–1400.
443 https://doi.org/10.1007/978-3-319-09048-1_57

444 Sousa, L., Barabasch, J., Stein, K.J., Siegesmund, S., 2017. Characterization and quality assessment of
445 granitic building stone deposits: A case study of two different Portuguese granites. *Eng. Geol.* 221,
446 29–40. <https://doi.org/10.1016/j.enggeo.2017.01.030>

447 Sousa, L.M.O., Oliveira, A.S., Alves, I.M.C., 2016. Influence of fracture system on the exploitation of
448 building stones: the case of the Mondim de Basto granite (north Portugal). *Environ. Earth Sci.* 75, 39.
449 <https://doi.org/10.1007/s12665-015-4824-6>

450 Taboada, J., Vaamonde, A., Saavedra, A., 1999. Evaluation of the quality of a granite quarry. *Eng. Geol.*
451 53, 1–11. [https://doi.org/10.1016/s0013-7952\(98\)00074-x](https://doi.org/10.1016/s0013-7952(98)00074-x)

452 Taboada, J., Vaamonde, a., Saavedra, a., Alejano, L., 1997. Application of geostatistical techniques to
453 exploitation planning in slate quarries. *Eng. Geol.* 47, 269–277. [https://doi.org/10.1016/S0013-](https://doi.org/10.1016/S0013-7952(97)00024-0)
454 [7952\(97\)00024-0](https://doi.org/10.1016/S0013-7952(97)00024-0)

455 Tercan, A.E., Özçelik, Y., 2000. Geostatistical evaluation of dimension-stone quarries. *Eng. Geol.* 58, 25–
456 33. [https://doi.org/10.1016/S0013-7952\(00\)00048-X](https://doi.org/10.1016/S0013-7952(00)00048-X)

457 Tomasic, I., 1994. The influence of discontinuity fabric and other factors on optimum exploitation of
458 dimension stone. *Rud. Zb.* 6, 101–105.

459 Turanboy, A., 2010. A geometric approach for natural rock blocks in engineering structures. *Comput.*
460 *Geosci.* 14, 565–577. <https://doi.org/10.1007/s10596-009-9171-9>

461 Turanboy, A., Ülker, E., 2008. LIP-RM: An attempt at 3D visualization of in situ rock mass structures.
462 *Comput. Geosci.* 12, 181–192. <https://doi.org/10.1007/s10596-007-9077-3>

463 Ülker, E., Turanboy, A., 2009. Maximum volume cuboids for arbitrarily shaped in-situ rock blocks as
464 determined by discontinuity analysis—A genetic algorithm approach. *Comput. Geosci.* 35, 1470–
465 1480. <https://doi.org/10.1016/j.cageo.2008.08.017>

466 Yarahmadi, R., Bagherpour, R., Kakaie, R., Mirzaie, N.H., Yari, M., 2014. Development of 2D computer
467 program to determine geometry of rock mass blocks. *Int. J. Min. Sci. Technol.* 24, 191–194.
468 <https://doi.org/10.1016/j.ijmst.2014.01.008>

469 Yarahmadi, R., Bagherpour, R., Khademian, A., Mirzaie, H., Kakaie, R., 2015. Developing a Matlab code
470 for determine geometry of rock mass blocks and its application in mining and rock mechanic
471 engineering. *J. Min. Metall.* 51A, 41–49. <https://doi.org/10.5937/JMMA1501041Y>

472 Yarahmadi, R., Bagherpour, R., Khademian, A., Sousa, L.M.O., Almasi, S.N., Esfahani, M.M., 2017.

473 Determining the optimum cutting direction in granite quarries through experimental studies: a case
474 study of a granite quarry. Bull. Eng. Geol. Environ. <https://doi.org/10.1007/s10064-017-1158-5>

475 Yarahmadi, R., Bagherpour, R., Taherian, S.-G., Sousa, L.M.O., 2018. Discontinuity modelling and rock
476 block geometry identification to optimize production in dimension stone quarries. Eng. Geol. 232,
477 22–33. <https://doi.org/10.1016/j.enggeo.2017.11.006>

478

479

480

481

482

483

484

485

486

487

488

489

490

491

492

493

494

495

496

497

498

Appendix A

499 The input parameter file (BlockCutOpt.par) in BlockCutOpt program for stratum a in the case study of
500 limestone quarry, considering the non-division of the tested area.

```
#BlockCutOpt parameters file
x_max=+27.00 #
x_min=+0.0 #
y_max=+65.00 #comment
y_min=+0.0 #comment
z_max=0.8 #
z_min=0.0 #comment
psi_max=3.1416 #
psi_step=0.0523598775598299 #
dx_step=0.5 #
dy_step=0.5 #
dim_block_x=3.025 #
dim_block_y=2.025 #
dim_block_z=0.825 #
mx=1
my=1
read_bound=0 #
BiDimensional=0 #
material-lost-by-quarrying =0.05 #
read_block_dimension=1 #
write_vtu=2 #
rotation_method=1 #
read_PLY_FileList=1 #
end=end
```

501
502

503

504

505

506

507

508

509

510

511

512

513

514

515

Appendix B

516 The input parameter file (BlockCutOpt.par) in BlockCutOpt program for the case study of the large scale
517 granite quarrying area, considering the sub-division of the tested area (mx=6,my=3).

518

```
#BlockCutOpt parameters file
x_max=+31070.80449 #
x_min=+25397.77196 #
y_max=+10723.88741 #comment
y_min=+5007.604247 #comment
z_max=6.00 #
z_min=0.0 #comment
psi_max=3.1416 #
psi_step=0.0523598775598299 #
dx_step=7.0 #
dy_step=5.0 #
dim_block_x=21.025 #
dim_block_y=9.025 #
dim_block_z=6.025 #
mx=3
my=2
read_bound=0 #
BiDimensional=1 #
material-lost-by-quarrying=0.05 #
read_block_dimension=1 #
write_vtu=2 #
rotation_method=1 #
read_PLY_FileList=1 #
end=end
```

519